

Modeling Photochemical [4 + 4] Cycloadditions: Conical Intersections Located with CASSCF for Butadiene + Butadiene

Michael J. Bearpark,[†] Merce Deumal,^{†,‡} Michael A. Robb,^{*,†} Thom Vreven,[†]
Naoko Yamamoto,[†] Massimo Olivucci,^{*,§} and Fernando Bernardi[§]

Contribution from the Department of Chemistry, King's College London, Strand, London WC2R 2LS, U.K., and Dipartimento di Chimica 'G. Ciamician' dell' Università di Bologna, Via Selmi 2, 40126 Bologna, Italy

Received July 25, 1996[⊗]

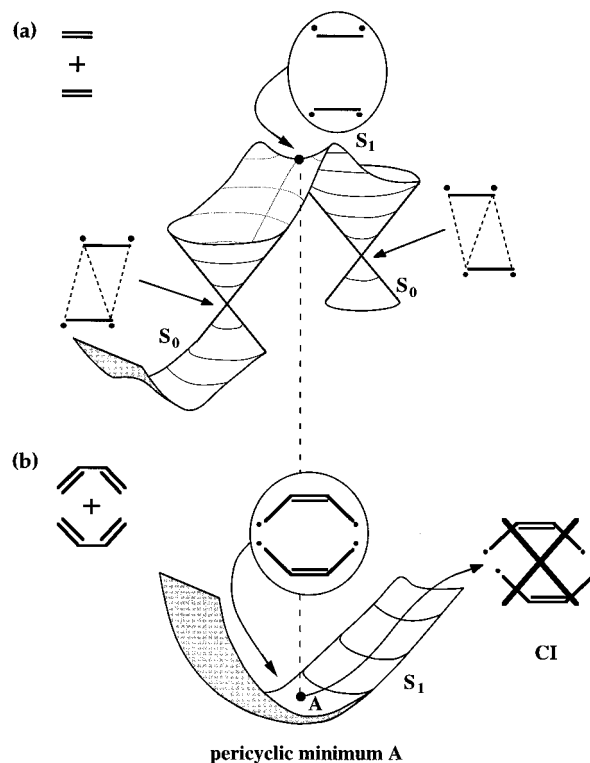
Abstract: The [4 + 4] photocycloaddition of butadiene + butadiene has been studied at the CASSCF/4-31G level, as a prototype for a class of photochromic systems. For this model system, minima and transition structures are characterized by analytic frequency calculations, and conical intersections are located. Our results indicate that the standard model for the [4 + 4] addition (based on H₄) needs to be revised. The reorganization of all 8π electrons is crucial (i.e., it is not always the same 4π electrons that are important). Efficient nonradiative decay of butadiene + butadiene can be explained by the presence of two distinct S₁/S₀ conical intersections. The first-the lowest-energy point on S₁ overall-is preceded by a barrier for the formation of a new σ bond. The resulting structure is similar to those previously characterized for methyl migration in but-1-ene and the addition of ethylene to benzene. A higher-energy barrier leads to a second crossing which resembles the rhomboidal funnel for the [2 + 2] addition of ethylene + ethylene, but which involves only one double bond from each butadiene. Both reaction paths commence at a true pericyclic minimum, at which the (S₀–S₁) energy gap of ~37 kcal mol⁻¹ prohibits decay.

Introduction

The [4_s + 4_s] cycloaddition is thermally forbidden but photochemically allowed.^{1,2} In this work we shall consider the prototypical [4 + 4] cycloaddition of two butadienes which serves as a model for many examples of more complex [4 + 4] cycloadditions such as anthracene photodimerization.

In spite of the fact that one has a formal 8π electron process, it is usually assumed that only 4π electrons are actually involved in the recoupling process along the reaction path so that the reactivity can be rationalized in a similar fashion to the classic [2 + 2] cycloaddition. The conventional model for the [4 + 4] photocycloaddition process^{3a,2a,4} is based on VB calculations for the H₄ system³ (Figure 1) which indicated the presence of a pericyclic minimum in the region of S₁ corresponding to a doubly-excited state. This minimum is assumed to be the decay funnel for the photochemical process.⁵ However, the original H₄ calculations illustrate the problems with a symmetry constraint: the pericyclic minimum in Figure 1 is in fact a

Scheme 1



transition structure on a rhomboidal distortion coordinate^{3,6ab} which connects two lower-energy conical intersections.⁷ These intersections have since been characterized for the ethylene + ethylene system (Scheme 1a)^{6a,b} and provide an efficient mechanism for nonradiative decay to S₀.

The purpose of this paper is to examine the [4 + 4] addition of butadiene + butadiene⁸ as a model for general [4 + 4] cycloadditions. This model is small enough to permit full geometry optimization at the CASSCF level for minima,

[†] Department of Chemistry, King's College.

[§] Dipartimento di Chimica 'G. Ciamician' dell' Università di Bologna.

[‡] Permanent address, Departament de Química Física, Universitat de Barcelona, Martí i Franques, 1 08028 Barcelona.

[⊗] Abstract published in *Advance ACS Abstracts*, January 1, 1997.

(1) (a) Woodward, R. B.; Hoffmann, R. *Angew. Chem., Int. Ed. Engl.* **1969**, *8*, 781–852. (b) Woodward, R. B.; Hoffmann, R. *The Conservation of Orbital Symmetry*; Academic Press: New York, 1971.

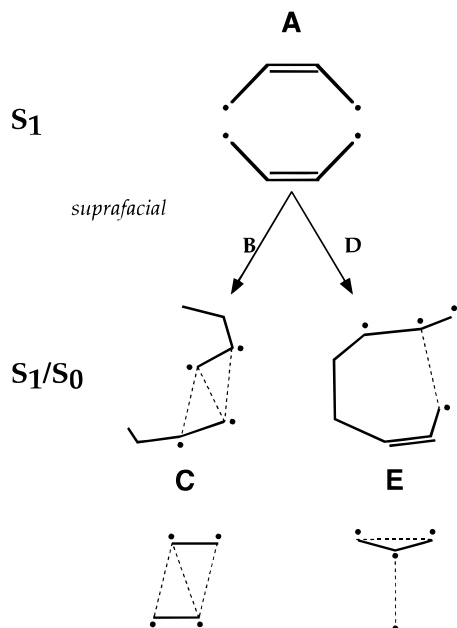
(2) For reviews of [4 + 4] cycloadditions, see: (a) Bouas-Laurent, H.; Desvergne, J.-P.; Chapter 14 In *Photochromism: Molecules and Systems*; Dürr, H., Bouas-Laurent, H., Eds.; Elsevier: Amsterdam, 1990. (b) Dilling, W. L. *Chem. Rev.* **1969**, *69*, 845–877. (c) Cowan, D. O.; Drisko, R. L. *Elements of Organic Photochemistry*; Plenum Press: New York, 1976; pp 388–480. (d) Turro, N. J. *Modern Molecular Photochemistry*; 1978. (e) Stevens, B. *Adv. Photochem.* **1971**, *8*, 161–226. (f) McCullough, J. J. *Chem. Rev.* **1987**, *87*, 811–860.

(3) (a) Michl, J. *Pure Appl. Chem.* **1975**, *41*, 507–534. (b) Gerhartz, W.; Poshusta, R. D.; Michl, J.; *J. Am. Chem. Soc.* **1976**, *98*, 6427–6443. (c) Gerhartz, W.; Poshusta, R. D.; Michl, J. *J. Am. Chem. Soc.* **1977**, *99*, 4263–4271.

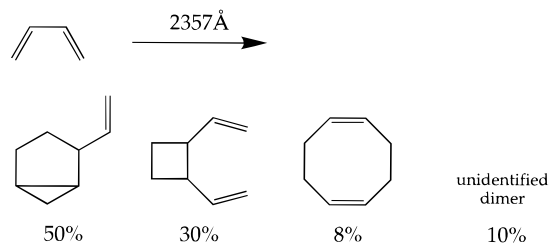
(4) Caldwell, R. A. *J. Am. Chem. Soc.* **1980**, *102*, 4004–4007.

(5) Van der Lugt, W. T. A. M.; Oosterhoff, L. J. *J. Am. Chem. Soc.* **1969**, *91*, 6042–6049.

Scheme 2



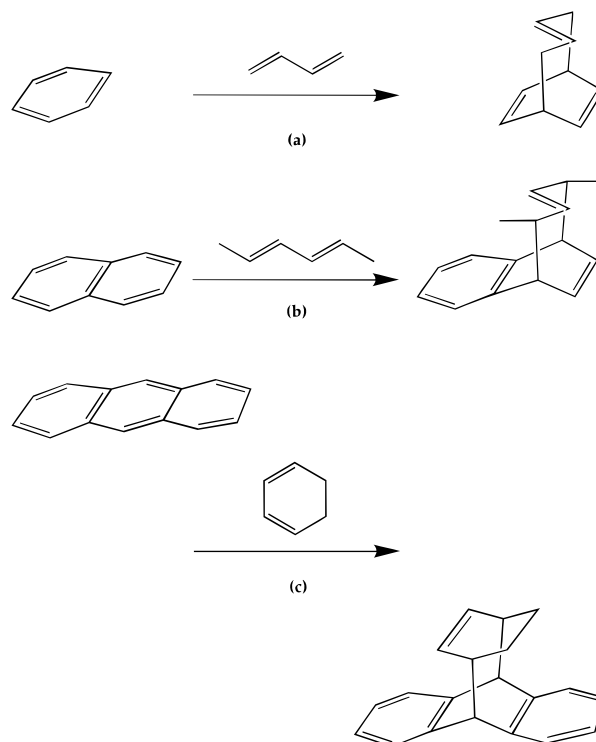
Scheme 3



transition structures, and conical intersections.⁶ We shall show that a model involving 4π electron recoupling is indeed adequate to describe $[4 + 4]$ photochemical processes and that the interesting regions of the potential energy surfaces for real $[4 + 4]$ systems will be determined by the constraints of the σ -bonded framework. However, the 4π electrons are not in general the same as for a $[2 + 2]$ reaction, and generalization of this model⁴ is not simple. For the ethylene + ethylene system (Scheme 1a), the pericyclic structure is a transition structure on S_1 that connects two rhomboid conical intersections. In contrast we find a true pericyclic $[4_s + 4_s]$ minimum **A** for butadiene + butadiene (Scheme 1b). Rhomboidal distortion does not lead to a surface crossing in this case. Rather, two reaction paths exist, commencing at the pericyclic minimum **A** and proceeding via low barriers to the conical intersections **C** ($[2_s + 2_s]$) and **E** ($[4 + 4]$) illustrated in Scheme 2.

(6) (a) Bernardi, F.; De, S.; Olivucci, M.; Robb, M. A. *J. Am. Chem. Soc.* **1990**, *112*, 1737–1744. (b) Bernardi, F.; Olivucci, M.; Robb, M. A. *Acc. Chem. Res.* **1990**, *23*, 405–412. (c) Bernardi, F.; Olivucci, M.; Robb, M. A.; Tonachini, G. *J. Am. Chem. Soc.* **1992**, *114*, 5805–5812. (d) Olivucci, M.; Ragazos, I. N.; Bernardi, F.; Robb, M. A. *J. Am. Chem. Soc.* **1993**, *115*, 3710–3721. (e) Celani, P.; Bernardi, F.; Olivucci, M.; Robb, M. A. *J. Chem. Phys.* **1995**, *102*, 5733–5742. (f) Olivucci, M.; Bernardi, F.; Ragazos, I.; Robb, M. A. *J. Am. Chem. Soc.* **1994**, *116*, 1077–1085. (g) Celani, P.; Ottani, S.; Olivucci, M.; Bernardi, F.; Robb, M. A. *J. Am. Chem. Soc.* **1994**, *116*, 10141–10151. (h) Celani, P.; Garavelli, M.; Ottani, S.; Bernardi, F.; Robb, M. A.; Olivucci, M. *J. Am. Chem. Soc.* **1995**, *117*, 11584–11585. (i) Palmer, I. J.; Ragazos, I. N.; Bernardi, F.; Olivucci, M.; Robb, M. A.; *J. Am. Chem. Soc.* **1993**, *115*, 673–682. (j) Bearpark, M. J.; Olivucci, M.; Wilsey, S.; Bernardi, F.; Robb, M. A. *J. Am. Chem. Soc.* **1995**, *117*, 6944–6953. (k) Bearpark, M. J.; Bernardi, F.; Clifford, S.; Olivucci, M.; Robb, M. A.; Smith, B. R.; Vreven, T. *J. Am. Chem. Soc.* **1996**, *118*, 169–175. (l) Bearpark, M. J.; Bernardi, F.; Olivucci, M.; Robb, M. A.; Smith, B. R. *J. Am. Chem. Soc.* **1996**, *118*, 5254–5260. (m) Clifford, S.; Bearpark, M. J.; Bernardi, F.; Olivucci, M.; Robb, M. A.; Smith, B. R. *J. Am. Chem. Soc.* **1996**, *118*, 7353–7360.

Scheme 4



The electronic origin of the crossings **C** and **E** (Scheme 2) can be related to four-electron recoupling processes in other systems we have studied before.^{6a–c} Both **C** and **E** are tetrameroid, decay from which can lead to a mixture of products as there are several possibilities for electron recoupling on S_0 . The conical intersection **E** (Scheme 2) is the lowest-energy point on S_1 overall. One σ bond has already been formed, and the four radical centers are arranged in the manner of the conical intersection for methyl migration in but-1-ene shown at the bottom of Scheme 2. A similar crossing is found to be the global minimum of S_1 for the ethylene + benzene system.^{6m} The higher-energy crossing **C** resembles the one due the rhomboidal distortion in the H_4 system.³ One double bond participates from each butadiene molecule; the other spectates.

Little experimental information is available on the direct photochemical dimerization of butadiene + butadiene^{9,2b,10} (in contrast with the triplet sensitised reaction¹¹). This is due in part to the rapid unimolecular decay of photoexcited butadiene itself: Mathies has established¹² that crossing from the initially excited 1^1B_u state of butadiene to the reactive 2^1A_g state takes place on the same time scale as vibrational relaxation (~ 10 fs),^{6c}

(7) A conical intersection is an $(n-2)$ dimensional subspace of (n) nuclear coordinates in which two states are degenerate. Movement along the two remaining linearly-independent nuclear coordinates (the nonadiabatic coupling and gradient difference vectors) lifts the degeneracy. (a) Teller, E. *J. Phys. Chem.* **1937**, *41*, 109. (b) Kauzmann, W. *Quantum Chemistry*; Academic Press: New York, 1957; pp 696–697. (c) Barrow, G. M. *Introduction to Molecular Spectroscopy*; McGraw-Hill: New York, 1962; p 306. (d) Herzberg, G.; Longuet-Higgins, H. C. *Disc. Faraday. Soc.* **1963**, *35*, 77. (e) Herzberg, G. *The Electronic Spectra of Polyatomic Molecules*; Van Nostrand: Princeton, 1966; p 442. (f) Teller, E. *Isr. J. Chem.* **1969**, *7*, 227–235. (g) Longuet-Higgins, H. C. *Proc. Roy. Soc. London A* **1975**, *344*, 147–156. (h) Salem, L. *Electrons in Chemical Reactions: First Principles*; Wiley: New York, 1982; pp 148–153. (i) Bonacic-Koutecky, V.; Koutecky, J.; Michl, J. *Angew. Chem., Int. Ed. Engl.* **1987**, *26*, 170–189. (j) Keating, S. P.; Mead, C. A. *J. Chem. Phys.* **1987**, *86*, 2152–2160. (k) Mead, C. A. *Rev. Mod. Phys.* **1992**, *64*, 51–85. (l) Atchity, G. J.; Xantheas, S. S.; Ruedenberg, K. *J. Chem. Phys.* **1991**, *95*, 1862–1876. (m) Manthe, U.; Köppel, H. *J. Chem. Phys.* **1990**, *93*, 1658–1669. (n) Schon, J.; Köppel, H. *J. Chem. Phys.* **1995**, *103*, 9292–9303. (o) Klessinger, M. *Angew. Chem., Int. Ed. Engl.* **1995**, *34*, 549–551.

(8) Salem, L. *J. Am. Chem. Soc.* **1968**, *90*, 553–556.

Table 1. Energies of the Optimized CASSCF/4-31G Structuresⁱ

structure	figure	active space	S_0, E_h	S_1, E_h	$\Delta E(S_1 - S_0)$ kcal mol ⁻¹	ΔE on S_1^a kcal mol ⁻¹
M ^b A	4a	8	-309.41640	-309.35697	37.2	0.0
∞^c	4b	8	-309.45948	-309.33163	80.2	+15.9
TS B	5a	8	-309.40673	-309.33265	46.5	+15.3
TS D	5b	8	-309.43917	-309.34206	60.9	+9.4
X C	6a	8	-309.34337 ^h	-309.34302 ^h	0.2	+8.8
X E	6b	6	-309.35710 ^h	-309.35706 ^h	0.03	
		8 CI (6) ^d	-309.37377 ^h	-309.37364 ^h	0.08	
		8	-309.37396 ^h	-309.37379 ^h	0.1	-10.6 ^e
X C _{tc} ^f	7a	8	-309.34121 ^h	-309.34047 ^h	0.5	+10.4
X E _{tc}	7b	6	-309.35553 ^h	-309.35450 ^h	0.6	
		8 CI (6) ^d	-309.37182 ^h	-309.37048 ^h	0.8	
		8	-309.37198 ^h	-309.37063 ^h	0.8	-8.6
M	8	8	-309.44176	-309.34198	62.6	+9.4
X	12	4	-309.23452 ^h	-309.23371 ^h	0.5	
		8 CI (4) ^d	-309.26611 ^h	-309.26531 ^h	0.5	
		8	-309.26850 ^h	-309.26722 ^h	0.5	+56.3
M/S ₀ ^g	14a	4	-309.49270			
		8 CI (4) ^d	-309.52436			
		8	-309.52513			
∞/S_0	14b	8	-309.51141			
M/S ₀	15	4	-309.46446			
		8 CI (4) ^d	-309.49857			
		8	-309.49893			

^a Energy on S_1 relative to pericyclic minimum **A**. ^b M = minimum; TS = transition structure; X = conical intersection. ^c Separation 10 Å. ^d m CI (n) indicates an m-orbital CASSCF calculation carried out with orbitals optimized for a n-orbital active space. ^e Relative energies calculated with the CAS8 active space. ^f tc = trans + cis suprafacial approach. ^g All structures optimized on S_1 , unless indicated by / S_0 . ^h State-averaged orbitals. ⁱ Analytic frequency calculations carried out for **4a**, **5a**, **5b**, and **8**. The minimum **8** and transition structure **5b** are almost coincident.

Table 2. CASSCF/6-31G* Energies at the Optimized CASSCF/4-31G Structures on S_1

structure	figure	active space	S_0, E_h	S_1, E_h	$\Delta E(S_1 - S_0)$ kcal mol ⁻¹	ΔE on S_1^a kcal mol ⁻¹
M ^b A	4a	8		-309.78750		0.0
∞^c	4b	8		-309.76193		+16.0
TS B	5a	8		-309.76336		+15.1
TS D	5b	8		-309.77691		+6.6
X C	6a	8	-309.77776 ^f	-309.77067 ^f	4.4	+10.6
X E	6b	6	-309.79459 ^f	-309.79286 ^f	1.1	
		8 CI (6) ^d	-309.81067 ^f	-309.80890 ^f	1.1	-13.4 ^e
		4	-309.69086 ^f	-309.68443 ^f	3.9	
X	12	8 CI (4) ^d	-309.72120 ^f	-309.71453 ^f	4.2	+45.8

^a Energy on S_1 relative to pericyclic minimum **A**. ^b M = minimum; TS = transition structure; X = conical intersection. ^c Separation 10 Å. ^d m CI (n) indicates an m-orbital CASSCF calculation carried out with orbitals previously optimized for a n-orbital active space. Full optimization at 6-31G* not attempted, as this led only to a further <0.1 kcal mol⁻¹ reduction in energy at the 4-31G level. ^e Relative energies calculated with the CAS8 active space. ^f State-averaged orbitals.

and 2^1A_g subsequently decays to the ground state on the picosecond time scale because of the presence of a twisted conical intersection.^{6d} This means that the concentration of excited butadiene will always be small, and collisions involving an excited molecule will be unlikely. Nevertheless, low dimerization yields were measured.^{9a,c,d} Yields for structures identified from the reaction in solution^{9c} are given in Scheme 3.

Shortly after the photochemical dimerization of butadiene was documented, it was discovered that dienes expedited the nonradiative decay of aromatic molecules.^{13a} A reaction profile, shown in Figure 1, involving excimer intermediates^{3,13,14} was suggested, but neither excimer emission nor products were detected at the time.^{13a,14f} Extensive work has since been carried

out on the photochemical addition of butadiene to benzene,¹⁵ naphthalene,¹⁶ and anthracene¹⁷⁻¹⁹ (Scheme 4).

Products have been characterized, and the formation of strained *trans*-diene adducts taken to indicate that the reaction is concerted.^{17a,f} (The product structure reflects the dominant ground state conformer of the diene,²⁰ ^{11c} not the most stable

(9) (a) Srinivasen, R. *J. Am. Chem. Soc.* **1960**, *82*, 5063-5066. (b) Haller, I.; Srinivasen, R. *J. Chem. Phys.* **1964**, *40*, 1992-1997. (c) Srinivasen, R.; Sonntag, F. I. *J. Am. Chem. Soc.* **1965**, *87*, 3778-3779. (d) Srinivasen, R.; *Advan. Photochem.* **1966**, *4*, 113-142. (e) Srinivasen, R. *J. Am. Chem. Soc.* **1968**, *90*, 4498-4499. (f) Hammond, G. S. In *Reactivity of the Photoexcited Organic Molecule*; Interscience: New York, 1967; pp 129-136. (g) Bahurel, Y. L.; McGregor, D. J.; Penner, T. L.; Hammond, G. S. *J. Am. Chem. Soc.* **1972**, *94*, 637-638.

(10) Reference 2d, p 422.

(11) (a) Hammond, G. S.; Turro, N. J.; Fischer, A. *J. Am. Chem. Soc.* **1961**, *83*, 4674-4675. (b) Hammond, G. S.; Turro, N. J.; Lui, R. S. H. *J. Org. Chem.* **1963**, *28*, 3297-3303. (c) Liu, R. S. H.; Turro, N. J.; Hammond, G. S. *J. Am. Chem. Soc.* **1965**, *87*, 3406-3412. (d) DeBoer, C. D.; Turro, N. J.; Hammond, G. S. *Org. Syn.* **1967**, *47*, 64. (e) Lui, R. S. H.; Gale, D. M. *J. Am. Chem. Soc.* **1968**, *90*, 1897-1899. (f) Vesley, G. F.; Hammond, G. S. *Mol. Photochem.* **1973**, *5*, 367. (g) Mella, M.; Fasani, E.; Albin, A. *Tetrahedron* **1991**, *47*, 3137-3154.

(12) Trulson, M. O.; Mathies, R. *J. Phys. Chem.* **1990**, *94*, 5741.

(13) (a) Stephenson, L. M.; Whitten, D. G.; Vesley, G. F.; Hammond, G. S. *J. Am. Chem. Soc.* **1966**, *88*, 3665-3666, 3893. (b) Weller, A. *Pure Appl. Chem.* **1968**, *16*, 115-123. (c) Stephenson, L. M.; Hammond, G. S. *Pure Appl. Chem.* **1968**, *16*, 125-136. (d) Stephenson, L. M.; Hammond, G. S. *Angew. Chem., Int. Ed. Engl.* **1969**, *8*, 261-270.

(14) (a) Taylor, G. N. *Chem. Phys. Lett.* **1971**, *10*, 355-360. (b) Evans, T. R. *J. Am. Chem. Soc.* **1971**, *93*, 2081-2082. (c) Labianca, D. A.; Taylor, G. N.; Hammond, G. S. *J. Am. Chem. Soc.* **1972**, *94*, 3679-3683. (d) Taylor, G. N.; Hammond, G. S. *J. Am. Chem. Soc.* **1972**, *94*, 3684-3686. (e) Taylor, G. N.; Hammond, G. S. *J. Am. Chem. Soc.* **1972**, *94*, 3687-3692. (f) Caldwell, R. A.; Creed, D. *Acc. Chem. Res.* **1980**, *13*, 45.

product). The nature of any intermediates such as excimers is unclear,^{14f} as product formation might account for deactivation.^{18a} However, excimer emission has been detected in the diene + anthracene system^{17c,d} (following indirect kinetic evidence for diene + naphthalene^{14c-e}) and is well established in the dimerization of anthracene,²¹ the prototype for photochromic systems.^{2a}

Previous theoretical work on the [4 + 4] reaction has been focused on the function of the excimer.^{8,22,4} In this paper, we concentrate on understanding the nonradiative decay channels for the model system butadiene + butadiene which involve conical intersections. These are consistent with the concerted nature of the [4 + 4] reaction in real systems¹⁵⁻¹⁹ and with the limited experimental evidence for the formation of mixtures of products in butadiene + butadiene itself.⁹

Computational Details

The choice of active space is the most critical feature of a CASSCF calculation. For two planar butadiene molecules which are well-separated, the active space should consist of eight valence π orbitals for covalent excited state calculations. However, the formation of a new σ -bond will lead to a pair of redundant active orbitals (one doubly occupied and the other unoccupied) and poor CASSCF convergence.

(15) (a) Koltzenburg, G.; Kraft, H. *Angew. Chem., Int. Ed. Engl.* **1965**, *4*, 981-982. (b) Koltzenburg, G.; Kraft, H. *Tetrahedron Lett.* **1966**, 389-395. (c) Kraft, H.; Koltzenburg, G. *Tetrahedron Lett.* **1967**, 4357-4362. (d) Yang, N. C.; Libman, J. *Tetrahedron Lett.* **1973**, 1409-1412.

(16) (a) Kraft, H.; Koltzenburg, G. *Tetrahedron Lett.* **1967**, 4723-4728. (b) Yang, N. C.; Libman, J.; Savitzky, M. F. *J. Am. Chem. Soc.* **1972**, *94*, 9226-9227. (c) Yang, N. C.; Libman, J.; *J. Am. Chem. Soc.* **1972**, *94*, 9228-9229. (d) Mak, K. T.; Srinivasachar, J.; Yang, N. C. *J. Chem. Soc., Chem. Commun.* **1979**, 1038-1040. (e) Encinas, M. V.; Lissi, E. A. *J. Photochem.* **1985**, *29*, 385-395. (f) Kimura, M.; Sagara, S.; Morosawa, S. *J. Org. Chem.* **1982**, *47*, 4344-4347.

(17) (a) Yang, N. C.; Libman, J. *J. Am. Chem. Soc.* **1972**, *94*, 1405-1406. (b) Yang, N. C.; Libman, J.; Barrett, L.; Hui, M. H.; Loesch, R. L. *J. Am. Chem. Soc.* **1972**, *94*, 1406-1408. (c) Yang, N. C.; Shold, D. M.; McVey, J. K. *J. Am. Chem. Soc.* **1975**, *97*, 5004-5005. (d) Yang, N. C.; Srinivasachar, K.; Kim, B.; Libman, J. *J. Am. Chem. Soc.* **1975**, *97*, 5006-5008. (e) Yang, N. C.; Shold, D. M. *J. Chem. Soc., Chem. Commun.* **1978**, 978. (f) Yang, N. C.; Yates, R. L.; Masnovi, J.; Shold, D. M.; Chiang, W. *Pure Appl. Chem.* **1979**, *51*, 173-180. (g) Yang, N. C.; Shou, H.; Wang, T.; Masnovi, J. *J. Am. Chem. Soc.* **1980**, *102*, 6652-6654. (h) Yang, N. C.; Masnovi, J.; Chiang, W.; Wang, T.; Shou, H.; Yang, D. D. H. *Tetrahedron* **1981**, *37*, 3285-3300. (i) Wang, T. Y.; Ni, J. D.; Masnovi, J.; Yang, N. C. *Tetrahedron Lett.* **1982**, 1231-1234. (j) Kaupp, G.; Grüter, H.-W. *Angew. Chem., Int. Ed. Engl.* **1972**, *11*, 313-314. (k) Kaupp, G.; Grüter, H.-W. *Angew. Chem., Int. Ed. Engl.* **1972**, *11*, 718. (l) Kaupp, G.; Grüter, H.-W. *Angew. Chem., Int. Ed. Engl.* **1975**, *14*, 491-492. [m] Kaupp, G.; Teufel, E. *Chem. Ber.* **1980**, *113*, 3669-3674. [n] Kaupp, G.; Grüter, H.-W.; Teufel, E. *Chem. Ber.* **1983**, *116*, 630-644.

(18) (a) Saltiel, J.; Townsend, D. E. *J. Am. Chem. Soc.* **1973**, *95*, 6140-6142. (b) Saltiel, J.; Marchand, G. S.; Smothers, W. K.; Stout, S. A.; Charlton, J. L. *J. Am. Chem. Soc.* **1981**, *103*, 7159-7164. (c) Smothers, W. K.; Meyer, M. C.; Saltiel, J. *J. Am. Chem. Soc.* **1983**, *105*, 545-555. (d) Saltiel, J.; Dabestani, R.; Schanze, R.; Trojan, D.; Townsend, D. E.; Goedken, V. L. *J. Am. Chem. Soc.* **1986**, *108*, 2674-2687. (e) Smothers, W. K.; Saltiel, J. *J. Am. Chem. Soc.* **1983**, *105*, 2794-2799. (f) Charlton, J. L.; Dabestani, R.; Saltiel, J. *J. Am. Chem. Soc.* **1983**, *105*, 3473-3476. (g) Saltiel, J.; Dabestani, R.; Sears, D. F.; McGowan, W. M.; Hilinski, E. F. *J. Am. Chem. Soc.* **1995**, *117*, 9129-9138.

(19) Chang, S. L. P.; Schuster, D. I. *J. Phys. Chem.* **1987**, *91*, 3644-3649.

(20) (a) Forbes, W. F.; Shilton, R.; Balasubramanian, A. *J. Org. Chem.* **1964**, *29*, 3527-3531. Ratio of *trans:cis* butadiene at RTP = 96:4. (b) Smith, W. B.; Massingill, J. L. *J. Am. Chem. Soc.* **1961**, *83*, 4301-4302.

(21) (a) Chandross, E. A. *J. Chem. Phys.* **1965**, *43*, 4175. (b) Menter, J.; Förster, Th. *Photochem. Photobiol.* **1972**, *15*, 289. (c) Ferguson, J.; Mau, A. W.-H. *Mol. Phys.* **1974**, *27*, 377. (d) McVey, J. K.; Shold, D. M.; Yang, N. C. *J. Chem. Phys.* **1976**, *65*, 3375. (e) Bergmark, W. R.; Jones, G.; Reinhardt, T. E.; Halpern, A. M. *J. Am. Chem. Soc.* **1978**, *100*, 6665-6673. (f) Vala, M. T.; Hillier, I. H.; Rice, S. A.; Jortner, J. *J. Chem. Phys.* **1966**, *44*, 23-25. (g) Koutecky, J.; Paldus, J. *Theor. Chim. Acta* **1963**, *1*, 268.

(22) (a) Bernardi, F.; Olivucci, M.; Robb, M. A. *J. Am. Chem. Soc.* **1992**, *114*, 1606-1616. (b) Bearpark, M. J.; Bernardi, F.; Olivucci, M.; Robb, M. A. *Chem. Phys. Lett.* **1994**, *217*, 513-519.

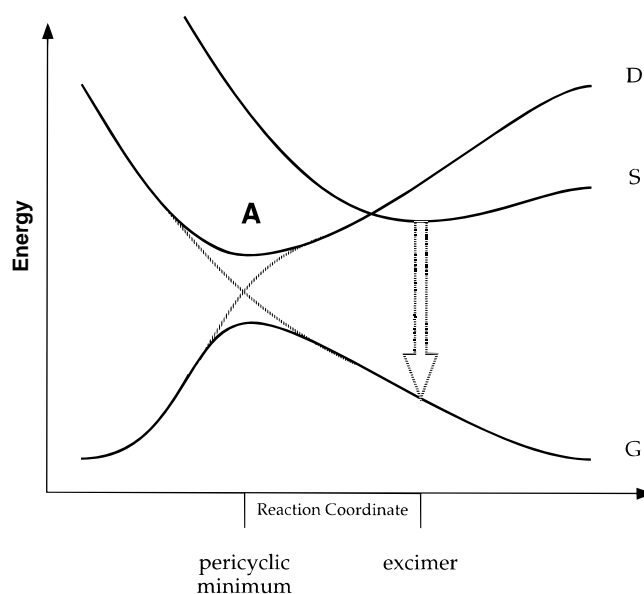


Figure 1. The conventional *model* potential energy curves for photochemical 2 + 2 or 4 + 4 cycloaddition, based on calculations for H₄.³ This symmetric cut shows an excimer minimum on the singly excited state S (which fluoresces in certain systems) and the pericyclic minimum A which results from an avoided crossing of the ground state G and doubly excited state D.

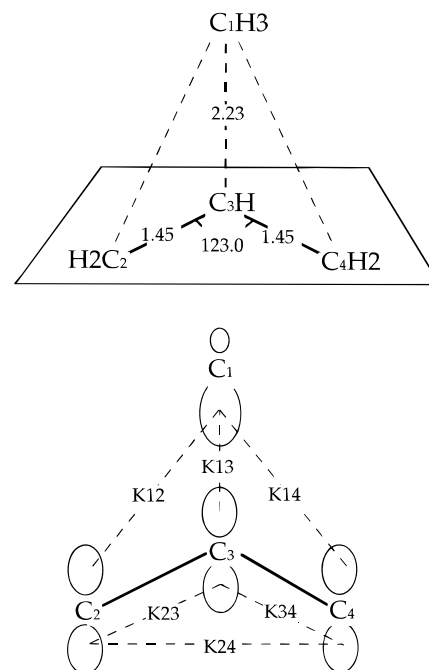


Figure 2. The prototype S_1/S_0 conical intersection in but-1-ene. In a simple VB model, the exchange integrals K_{ij} balance and the total exchange is zero at this geometry.

Redundant orbitals are therefore removed from the active space during geometry optimization but put back at the end for a final energy calculation.

MMVB²² structures were used as the starting point for CASSCF geometry optimizations.²³ Guess orbitals were derived²⁴ from stable

(23) Gaussian 94; Frisch, M. J.; Trucks, G. W.; Schlegel, H. B.; Gill, P. M. W.; Johnson, B. G.; Robb, M. A.; Cheeseman, J. R.; Keith, T. A.; Peterson, G. A.; Montgomery, J. A.; Raghavachari, K.; Al-Laham, M. A.; Zakrzewski, V. G.; Ortiz, J. V.; Foresman, J. B.; Cioslowski, J.; Stefanov, B. B.; Nanayakkara, A.; Challacombe, M.; Peng, C. Y.; Ayala, P. Y.; Chen, W.; Wong, M. W.; Andres, J. L.; Replogle, E. S.; Gomperts, R.; Martin, R. L.; Fox, D. J.; Binkley, J. S.; Defrees, D. J.; Baker, J.; Stewart, J. P.; Head-Gordon, M.; Gonzales, C.; Pople, J. A. Gaussian, Inc.: Pittsburgh, PA, 1995.

(24) Bofill, J. M.; Pulay, P. *J. Phys. Chem.* **1989**, *88*, 3637.

Table 3. Energies of the CASSCF/4-31G Antara Crossing Structures Shown in Figure 13

structure	figure	active space	S_0, E_h	S_1, E_h	$\Delta E(S_1 - S_0)$ kcal mol ⁻¹	ΔE on S_1 , ^a kcal mol ⁻¹
M^b A	5a	8	-309.41640	-309.35697	37.2	0.0
X C_s	13a	8	-309.24990 ^c	-309.24621 ^c	2.3	+69.5
X D_{2d}	13b	8	-308.94006 ^c	-308.93577 ^c	2.7	+264

^a Energy on S_1 relative to pericyclic minimum **A**. ^b M = minimum; X = conical intersection. ^c State-averaged orbitals.

UHF wave functions²⁵ New σ bonds were stretched to guarantee that the resulting active space could describe dissociation and that the final energetics would be comparable. The 4-31G basis used is sufficient to describe the topology of the S_1 surface, although polarization functions and an adequate treatment of dynamic electron correlation with geometry reoptimization would also be necessary to compute barrier heights accurately. Recomputing energies at the 6-31G* level does not change the barrier heights by more than ± 2 kcal mol⁻¹ unless the geometry is highly strained (e.g., **12** in Tables 1 and 2).

Saddle points were characterized by analytic second derivative calculations at the CASSCF/4-31G level of theory.²⁶ At these points, the single negative direction of curvature corresponds to the reaction coordinate. At a point on a conical intersection⁷ there are two linearly-independent nuclear coordinates—the nonadiabatic coupling and gradient difference vectors (branching space⁷¹)-which lift the degeneracy. The remaining directions define a space (intersection space⁷¹) in which the two states remain degenerate. Minima in the intersection space are located using the algorithm described in ref 27. Although decay can take place at any intersection point in principle, the region of the minimum will be favored when excess energy can be dissipated to the surroundings in condensed phases or when the system has very low excess energy such as cold jets. In these situations, the plane formed by the nonadiabatic coupling and gradient difference vectors will be the one in which initial motion on S_0 will take place. Furthermore, the gradient difference vector on S_1 will point along the reaction path.

Results and Discussion

A VB Model for the Crossing Geometries for Butadiene + Butadiene. A large body of experience suggests that conical intersections-funnels^{3a,28} at which decay can be fully efficient^{7m}—are most likely to occur at tetraradicaloid geometries.²⁹ A simple VB model^{6c,29} can be used to predict the existence of such intersections. The problem is then to determine which crossing geometries will be at low energy and accessible for a particular system. We now briefly outline some possibilities that can be predicted *a priori*.

According to a simple VB model,^{6c,29} a tetraradicaloid geometry corresponds to a conical intersection if the exchange integrals between the four different radicaloid centers balance. The condition for the exchange integrals (K_{ij}) is as follows:

$$K_{12} + K_{34} = K_{14} + K_{23} = K_{13} + K_{24}$$

The K_{ij} depend mainly on the overlap of the orbitals on sites i and j via the usual expression for the exchange integral in Heitler–London VB theory.

$$K_{ij} = \left\langle ij \left| \frac{1}{r_{12}} \right| ji \right\rangle + 2S_{ij} \langle i|h|j \rangle$$

where $\langle ij|1/r_{12}|ji \rangle$ is the exchange repulsion, $\langle i|h|j \rangle$ is the nuclear electron attraction integral, and S_{ij} is the overlap integral. Figure

(25) Seeger, R.; Pople, J. A. *J. Chem. Phys.* **1977**, *66*, 3045.

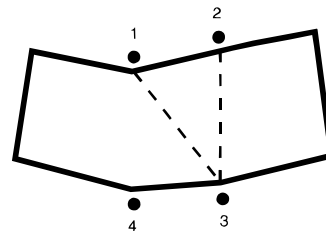
(26) Yamamoto, N.; Vreven, T.; Robb, M. A.; Frisch, M. J.; Schlegel, H. B. *Chem. Phys. Lett.* **1996**, *250*, 373–378.

(27) (a) Ragazos, I. N.; Robb, M. A.; Bernardi, F.; Olivucci, M. *Chem. Phys. Lett.* **1992**, *197*, 217–223. (b) Bearpark, M. J.; Robb, M. A.; Schlegel, H. B. *Chem. Phys. Lett.* **1994**, *223*, 269–274.

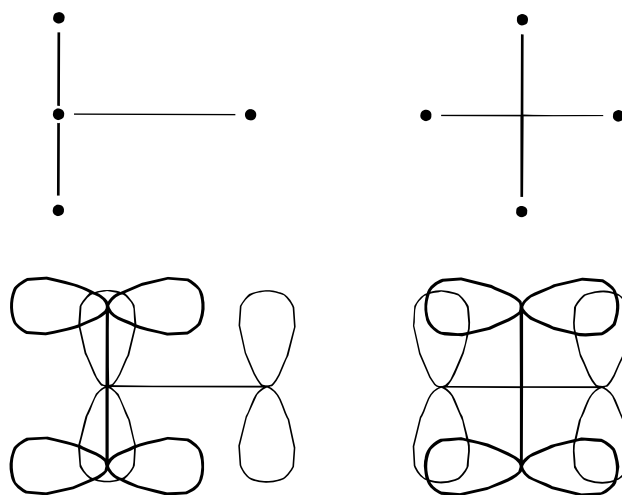
(28) Zimmerman, H. E. *J. Am. Chem. Soc.* **1966**, *88*, 1566–1567.

(29) Bernardi, F.; Olivucci, M.; Robb, M. A. *Isr. J. Chem.* **1993**, *33*, 265–276.

Scheme 5



Scheme 6



2 illustrates this situation for the but-1-ene^{6c} conical intersection. The first exchange equality is clearly satisfied by symmetry. The second can be fulfilled for certain values of the bond lengths and C–C–C angle. In butadiene + butadiene, the crossing **E** (Scheme 2) is of the but-1-ene type: one new σ bond has already been formed, and the four radical centers are drawn three from one butadiene, and one from another. Another crossing-**C** in Scheme 2—corresponds to the [2 + 2] addition of one double bond from each butadiene.^{6a,b} This crossing can be thought of as a balance of exchange integrals brought about by the close approach of two radical centers across the diagonal of the rhombus.

Both **C** and **E** correspond to crossing geometries identified in the H_4 system by Michl.³ Other tetraradicaloid geometries can be predicted, but these are disfavored in practice by framework strain or nonbonded repulsions.²⁹ One such geometry is shown in Scheme 5 for trans + cis butadiene, in which three close radical centers (labeled 1, 2, and 3) are distant from a fourth (labeled 4).

This is the $-(CH)_3-$ kink feature now recognized in polyenes^{6h} and aromatic systems benzene⁶ⁱ and styrene,^{6j} but, as we shall presently discuss, the framework distortion required to achieve this geometry in butadiene + butadiene places it unfavorably above the crossings **C** and **E** in energy.

Scheme 6 shows that the condition for zero total exchange can also be satisfied by the antara–antara approach of radical centers on the four terminal $-CH_2$ groups.

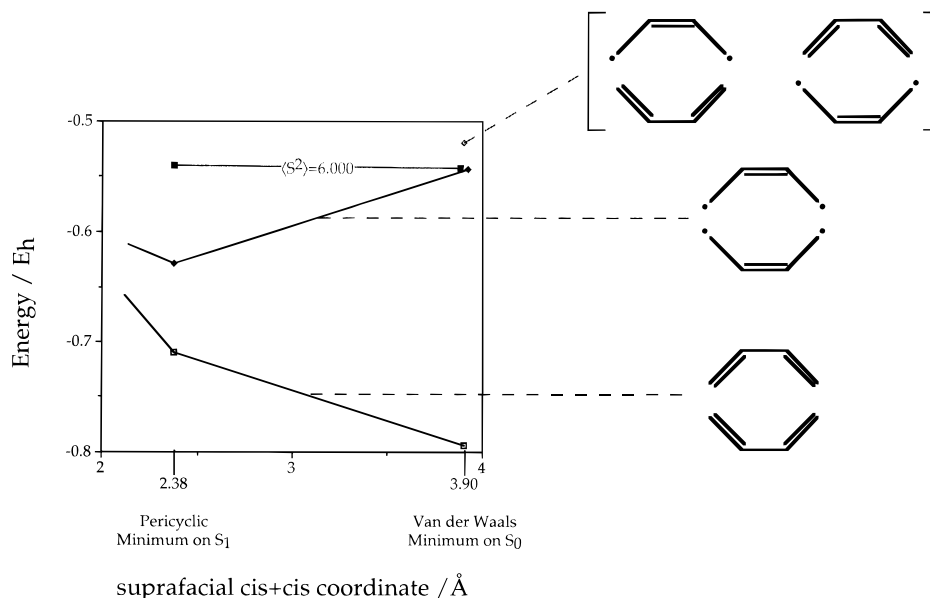


Figure 3. Electronic states of butadiene + butadiene along the cis + cis suprafacial reaction coordinate. Energies calculated with MMVB at the pericyclic minimum on S_1 and the van der Waals minimum on S_0 . At both geometries, S_1 corresponds to $D_A + D_B$ (i.e., 2^1A_g excitation in both butadienes). At the asymptotic limit (not shown) the $D_A + G_B$ state lies below the $D_A + D_B$ if the geometry is relaxed. However (see Table 1) if the geometry is fixed at that shown in Figure 4b, the $D_A + D_B$ state is S_1 .

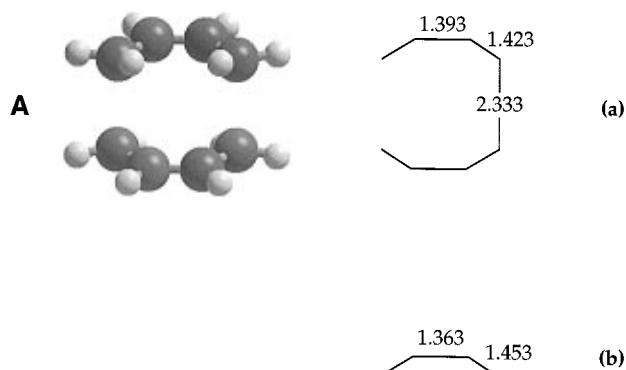


Figure 4. Optimized geometries for S_1 minima located with CASSCF/4-31G: **a** is the pericyclic minimum, and **b** is the isolated S_1 butadiene planar minimum.³¹ Energies in Table 1.

However, this difficult approach is excessively high in energy because of nonbonded repulsions, and we shall show that the antara-antara approach for the [4 + 4] reaction can be ruled out.

As we have suggested, the rhomboid supra-supra conical intersection involving the four terminal radical centers (Scheme 1b) does not exist.

The Pericyclic Minimum. Figure 3 shows the qualitative behavior of the covalent excited states along a cis-cis reaction path (computed with MMVB²²). It is convenient to classify these states according to the excited and ground states of butadiene: G_A, G_B (ground state S_0); S_A, S_B (corresponding to the singly excited 1B_u ionic state of trans butadiene); D_A, D_B (corresponding to the covalent doubly excited state 2^1A_g in trans butadiene); and T_A, T_B (corresponding to the triplet states 3B_u for trans butadiene). The central feature is the pericyclic minimum **A** on S_1 which correlates with two covalent doubly excited states $D_A + D_B$ or two triplet states $T_A + T_B$ of two butadienes at large internuclear separation in accord with the accepted model.⁴ Interactions between the four radical centres are attractive in butadiene + butadiene S_1 but repulsive in S_0 . The pericyclic minimum has been optimized at the CASSCF/4-31G level and is shown in Figure 4. The two butadiene molecules are 2.33 Å apart, and the inversion of single and

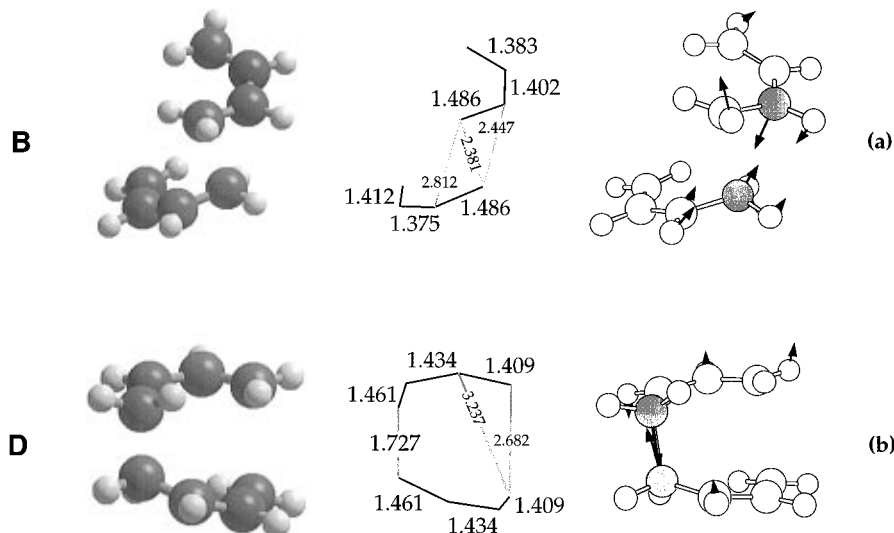


Figure 5. Optimized geometries for S_1 transition structures located with CASSCF/4-31G. Energies in Table 1.

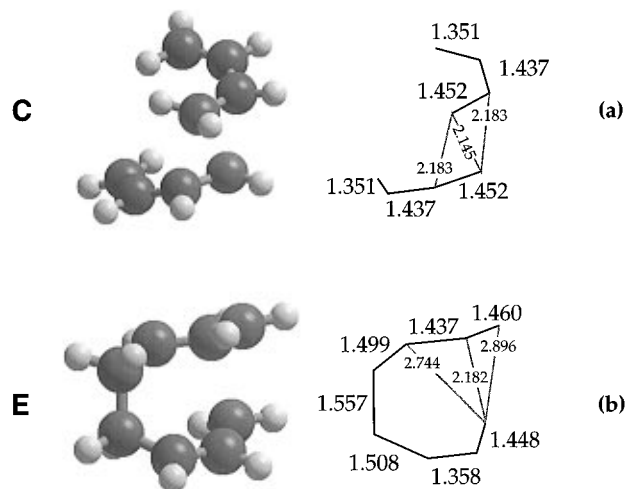


Figure 6. Optimized geometries for S_0/S_1 conical intersection minima located with CASSCF/4-31G. Energies in Table 1.

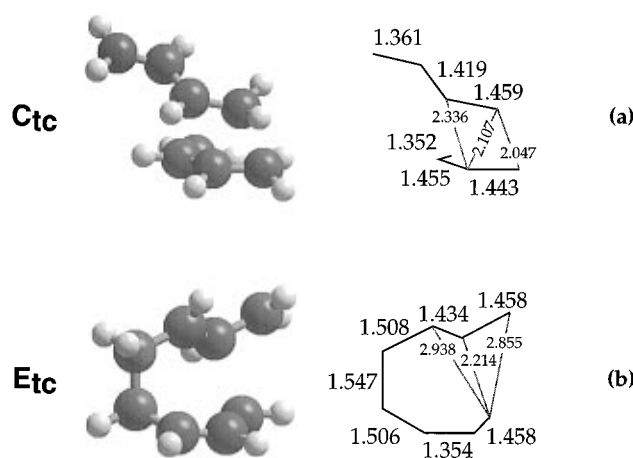


Figure 7. Optimized geometries for S_0/S_1 conical intersection minima located with CASSCF/4-31G: trans-cis isomers of the structures illustrated in Figure 6. Energies in Table 1.

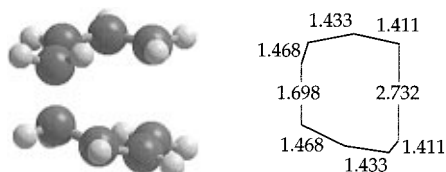


Figure 8. A minimum on S_1 at an almost identical geometry to the transition structure **D** in Figure 5.

double bonds within each butadiene is less extreme than for the isolated molecule in the planar 2^1A_g (D_A) minimum (**4b**).^{6d} A frequency calculation shows that **A** is a true minimum, with a binding energy of 16 kcal mol⁻¹ (Table 1). The S_1-S_0 gap at this geometry is 37 kcal mol⁻¹ (Table 1) which prohibits fast internal conversion.

Accurate calculations in the region where the two butadiene fragments are far apart are unreliable without the use of extended basis sets and are complicated by the existence of a state in which four unpaired spins are parallel: this lies below the $D_A + G_B$ state at large interfragment distance (see Figure 3). For butadiene itself, the S_1 covalent 2^1A_g state (D_A) lies above the 1B_u ionic state (S_A) in the vertical excitation region. However, rapid internal conversion to 2^1A_g has been shown to take place (~ 10 fs¹²). At a geometry of two S_0 butadienes which are 3.9 Å apart, the degenerate state corresponding to $D_A + G_B$ is already higher in energy than $D_A + D_B$. Thus the initial part of the reaction path lies outside the scope of the present

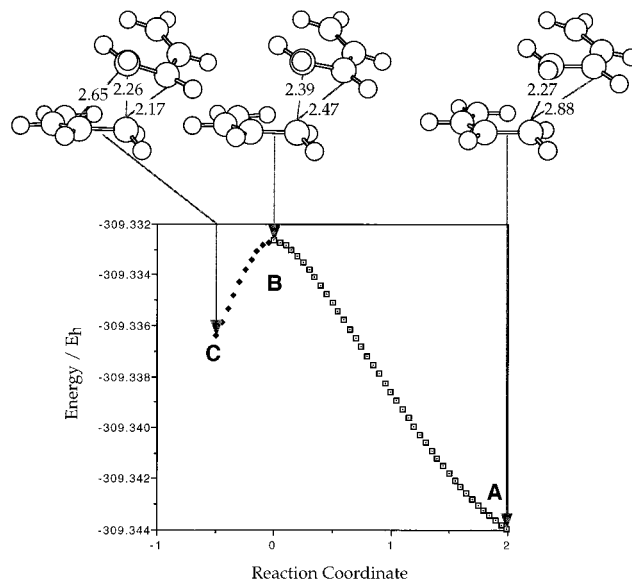


Figure 9. IRC in forward and reverse directions from the transition structure **B**.

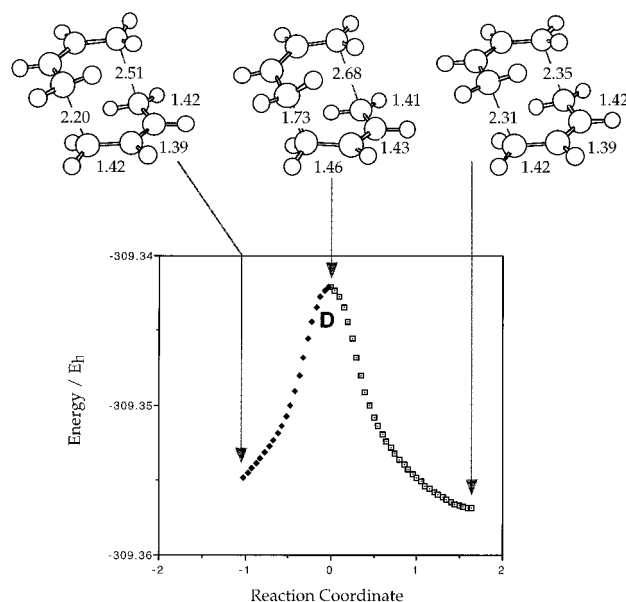


Figure 10. IRC in forward and reverse directions starting from the transition structure **D**.

investigation and the nature of any excimer minimum for butadiene + butadiene remains an open question.

Reaction Paths ABC and ADE Lead to Low Energy Crossings. Two reaction paths on S_1 have been characterized—**ABC** and **ADE** (Scheme 2)—which commence at the pericyclic minimum **A** and proceed via transition structures **B** and **D** (Figure 5) to (cis + cis) conical intersections **C** and **E** (Figure 6). Energies are given in Tables 1 (4-31G) and 2 (6-31G*). Trans + cis conical isomers (**C_{ct}** and **E_{ct}**) intersections **C** and **E** have also been optimized (Figure 7), but no trans + cis isomer minimum corresponding to **A** could be located.

The transition state **B** is calculated to be 15.3 kcal mol⁻¹ above **A**, less than 1 kcal mol⁻¹ below the dissociation limit (Table 1). Figure 5 shows that the corresponding transition vector is dominated by the formation of a new σ bond between the shaded centers. An IRC calculation from this point (Figure 9) demonstrates that this coordinate leads either back to **A** or forwards to a point on the S_1/S_0 crossing **C**.

The barrier height for coordinate **ADE** is 9.4 kcal mol⁻¹ (~ 6 kcal mol⁻¹ lower than that for **ABC**). The transition vector is

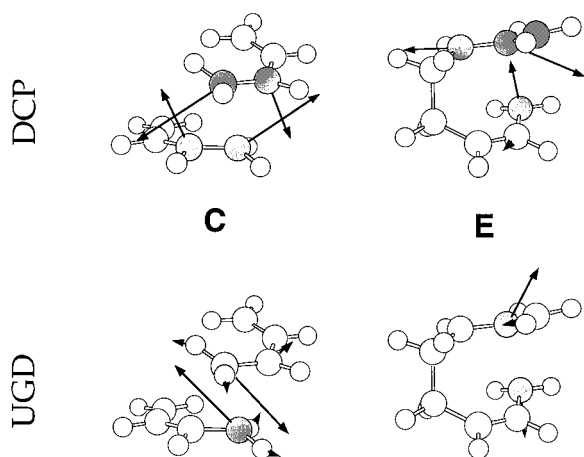


Figure 11. 11. The derivative coupling and gradient difference vectors—those which lift the degeneracy—computed with CASSCF/4-31G at the **C** and **E** crossings.

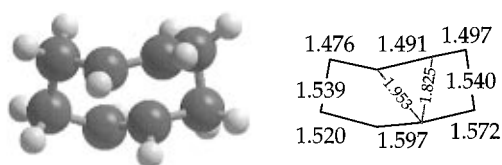


Figure 12. 12. A suprafacial trans–cis conical intersection optimized with CASSCF/4-31G, at higher energy (Table 1) than the crossings shown in Figures 6 and 7.

again dominated by the formation of a new σ -bond (Figure 5). However the transition state region is very flat. There is an additional distinct minimum (Figure 8) at a geometry close to **D**, with a slightly shorter σ -bond which has the same energy as the TS **D**. The fact that force constants are quite different at an almost identical geometry implies that the S_1 surface in this region is highly anharmonic. Quadratic force constants—including the transition vector—are of limited value. Thus an IRC calculations from this point is only partially successful (Figure 10). The reverse coordinate leads to the pericyclic minimum **A**, the IRC in “forwards” direction illustrated in Figure 10 actually decayed back toward **A**.

The crossing geometry **C** concurs with the simple VB model outlined above. The shortest interfragment separation is the 2.15 Å diagonal illustrated in Figure 6. One ethylene group from each butadiene participates; the other (bond length 1.35

Å) is almost unchanged from the ground state value for the isolated molecule (Figure 14.b). This crossing is 8.8 kcal mol⁻¹ above **A** (Table 1). The derivative coupling and gradient difference vectors at **C** are illustrated in Figure 11. These are the directions which lift the degeneracy, and, at low kinetic energies, initial motion on S_0 will take place in this plane. The two limiting motions (Figure 11) correspond to different ways of recoupling the four radical centers.³⁰ One direction leads to the formation of two new σ -bonds and hence a four-membered ring. The other leads to the π -bonds being reformed and return to isolated reactants. The relative yields of these two products will be a function of the nuclear dynamics.³¹

The crossing **E** is 10.6 kcal mol⁻¹ below **A**, 19.4 kcal mol⁻¹ below **C**, and the lowest energy point on S_1 overall (Table 1). Figure 6 shows that the closest approach on the opposite side of the new σ bond is 2.18 Å. Comparison with the transition structure in Figure 5 shows that a C_2 axis of symmetry has been lost: at some point on **ADE** after **D**, the reaction path must bifurcate to lead to two (equivalent) possible forms of **E**.

The directions which lift the degeneracy at **E** are shown in Figure 11. One points toward the formation of a seven-membered ring, the other is orthogonal, and combinations of the two could lead to six-, seven-, or eight-membered rings being formed initially. One of the surprises from the dynamics treatment of this problem³² (using MMVB²² to simulate the CASSCF potential) is that four-membered rings can also be formed after decay at this point. The existence of a conical intersection is therefore consistent with the experimental observation⁹ of a mixture of products, as indicated in Scheme 3. Note that alternate forms intermediate between **C** or **E** could also exist as precursors to a five-membered ring product. However these were not found in our work as minima on the conical intersection line. Rather, dynamics studies³² indicate that the five-membered ring product occurs from the conical intersection **E**.

—(**CH**)₃— **Kink and Antara–Antara Crossings.** Figure 12 shows that, in agreement with the VB prediction, a conical intersection can be formed by two butadienes as a result of interactions among the central four CH units (the —(**CH**)₃— kink conical intersection that exists in polyenes^{6h}). This crossing resembles **E**, but with two new σ bonds fully formed. There are two short cross-ring distances (1.95 Å and 1.83 Å), and one more distant radical center (as indicated in Scheme 5). However, in order to achieve this geometry, the σ framework

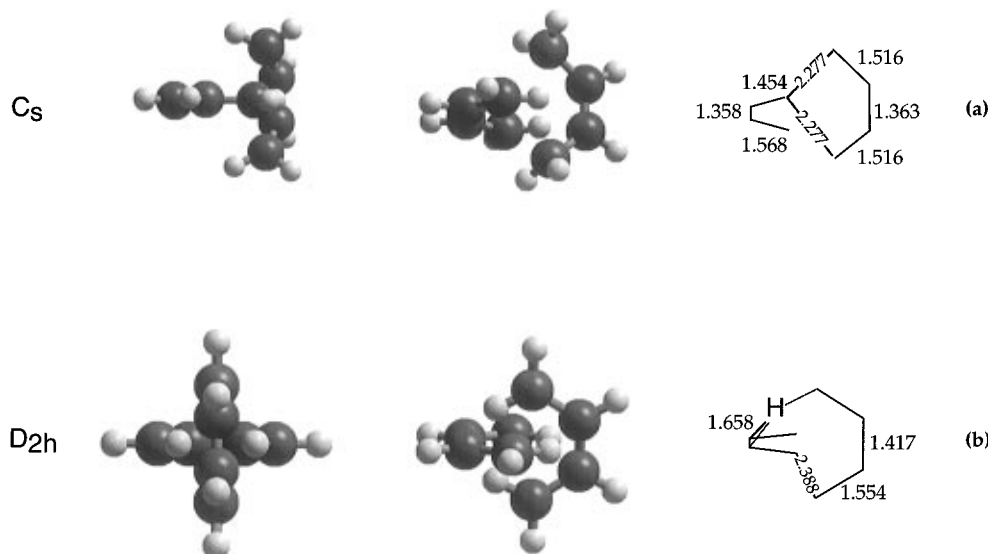


Figure 13. 13. Optimized geometries on the antara–antara S_1/S_0 conical intersection.

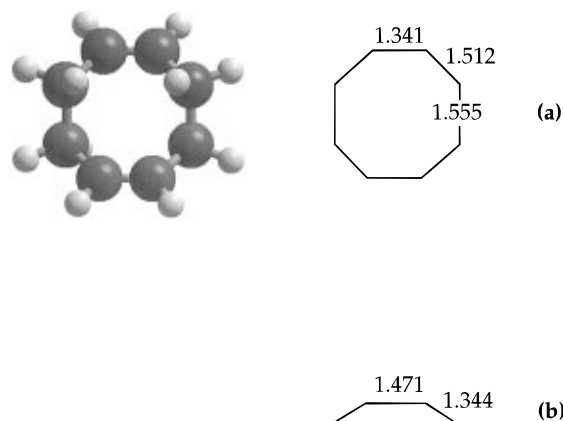


Figure 14. 14. Optimized geometries for S_0 minima located with CASSCF/4-31G: cyclooctatetraene **a** and isolated planar butadiene **b**. Energies in Table 1.

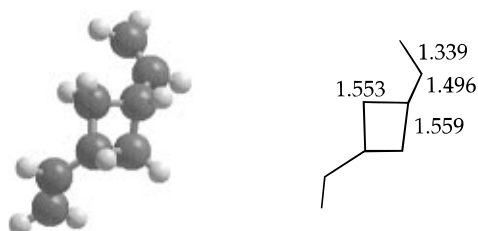


Figure 15. 15. Optimized geometries for S_0 minima located with CASSCF/4-31G: 1,3 divinylcyclobutane. Energies in Table 1.

has been strained considerably (e.g., bond lengths 1.60 Å, and angles $\ll 120^\circ$). This crossing is consequently over 50 kcal mol⁻¹ higher in energy than the pericyclic minimum (Table 1), although this high value is due in part to the lack of polarization functions in the 4-31G basis set used. Calculations at the 6-31G* level (Table 2) reduce the barrier by ~ 10 kcal mol⁻¹.

The conical intersection structure shown in Figure 12 is included because this type of interaction may be important in the addition of dienes to aromatic systems,¹⁵⁻¹⁹ in which the necessary distortions may be better accommodated by the σ framework than in butadiene. Scheme 4a,b show that the products of diene + aromatic photodimerization reflect the initial equilibrium of trans:cis isomers in the diene ground state,²⁰ which for butadiene is $\sim 96:4$.^{20b,11c} Although crossings **C** and **E** have been found to occur at trans + cis geometries (**C_{et}** and

E_{et} Figure 7) it may be that the Figure 12 crossing becomes competitive, as the radical centers can be efficiently delocalized.

Two points on a crossing located on the antara-antara path are illustrated in Figure 13. Table 3 shows that the large nonbonded repulsions place the lowest point on this crossing (Figure 13a, C_s geometry) at ~ 70 kcal mol⁻¹ above the pericyclic minimum **A**. This crossing is therefore unfavorable both energetically and entropically and can be disregarded unless a suitably constrained precursor geometry can be devised.

Products. Figures 14 and 15 illustrate two representative products on S_0 . Cyclooctadiene (**14a**) is calculated to be 95 kcal mol⁻¹ below the lowest point on the crossing **E** and 8.6 kcal mol⁻¹ below the dissociation limit on S_0 (Table 1). Kinetic energy must therefore be efficiently dissipated into the surrounding medium for this product to form. Figure 15 illustrates an isomer of 1,3-divinylcyclobutane, which is 98 kcal mol⁻¹ below the lowest point on the crossing **C** (Table 1). An interpolation along the path from **C** to 1,3-divinylcyclobutane is presented in Figure 16. The product is 7.8 kcal mol⁻¹ endothermic (Table 1) and may dissociate if the excess kinetic energy is not removed.

Conclusion

Two reaction paths **ABC** and **ADE** have been characterized on the S_1 excited state of the model butadiene + butadiene system. Both lead to a conical intersection, at which $S_1 \rightarrow S_0$ decay can be fully efficient. One intersection (**E**) is the lowest-energy point on S_1 overall.

The two conical intersections we have located for butadiene + butadiene can be related to intersections which have been characterized previously in conjugated hydrocarbons. This suggests that such intersections are quite general features of the excited states of these systems. At each crossing point (**C** and **E**), a mixture of products is predicted by examining the two coordinates which lift the degeneracy. The fact that there are two crossings in butadiene + butadiene-with different barrier heights-suggests that the product yields will be a complex function of experimental conditions. However, because of the efficient unimolecular decay of photoexcited butadiene, this study is intended principally to provide a general model for the [4 + 4] photocycloaddition. We have shown that it is not straightforward to generalize the model based on a highly-symmetric cut through the H_4 potential energy surfaces^{2a,3,4} in

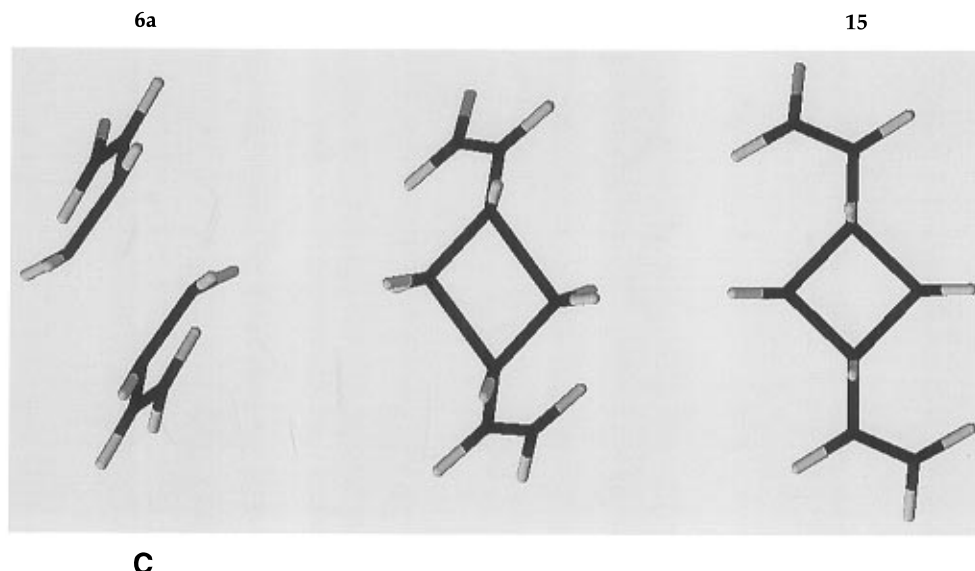


Figure 16. 16. A linear interpolation between the CASSCF/4-31G crossing geometry **6a** and the four-membered ring product **15**.

this case. The reason for this is that, although the conical intersections we have characterized for butadiene + butadiene can be related to features of the H_4 system,³ reorganization of all eight π electrons is crucial to produce those calculated to be favorable energetically (i.e., it is not always the same four electrons that are important). However, in contrast to the [2 + 2] addition^{3,6a,b} and in agreement with the simple model,²⁹ the pericyclic minimum is found to be a true minimum for butadiene + butadiene. The S_0 - S_1 energy gap of ~ 37 kcal mol⁻¹ prohibits decay at this point.

Our target in this work has been to document the excited

(30) Celani, P.; Robb, M. A.; Garavelli, M.; Bernardi, F.; Olivucci, M. *Chem. Phys. Lett.* **1995**, 243, 1-8.

(31) Smith, B. R.; Bearpark, M. J.; Robb, M. A.; Bernardi, F.; Olivucci, M. *Chem. Phys. Lett.* **1995**, 242, 27-32.

(32) Manuscript in preparation.

state surface topology for a model 4 + 4 cycloaddition. One may infer (from the geometry of the conical intersection and the nature of the gradient difference and derivative coupling vectors) that certain products may originate following decay at the conical intersections we have identified. However, the issue of product formation can only be answered as a result of dynamics studies³² which are required to fully understand the possible ways of recoupling the radical centers that occurs after decay at the conical intersection.

Acknowledgment. This research has been supported in part by the EPSRC (UK) under Grants GR/J25123 and GR/H58070. All CASSCF calculations were run on IBM RS/6000 using a development version of Gaussian.²³ Some images were created with MacMolecule © University of Arizona.

JA962576N